VOL. 19, NO. 23, DECEMBER 2024 ISSN 1819-6608
ARPN Journal of Engineering and Applied Sciences

www.arpnjournals.com

STRUCTURAL AND MAGNETIC PROPERTIES OF α-Fe_2O_3/TiO_2 NANOCOMPOSITE DERIVED FROM LOGAS NATURAL SAND FOR ENVIRONMENTAL APPLICATION

Erwin Amiruddin[1], Amir Awaluddin[2], Ari Sulistyo Rini[1], Dewi Natalia Hutahuruk[3], Miftahul Jannah[3]and Novalin Putri[4]
[1]Department of Physics, Faculty of Mathematics and Natural Sciences, Riau University, Pekanbaru, Indonesia
[2]Department of Chemistry, Faculty of Mathematics and Natural Sciences, Riau University, Pekanbaru, Indonesia
[3]Magnetic Laboratory, Faculty of Mathematics and Natural Sciences, Riau University, Pekanbaru, Indonesia
[4]Laboratorium Jalan, Civil Engineering Magister Study Program -Faculty of Civil Engineering, Diponegoro University, Semarang, Central Java, Indonesia
E-Mail: erwin.amiruddin@lecturer.unri.ac.id

ABSTRACT

In this study, the iron oxide/titanium dioxide (α-Fe_2O_3/TiO_2) nanocomposites were prepared by ball milling method using Logas natural sand as raw material. The effects of milling time on the structural, magnetic properties, and chemical composition of the sample were investigated using X-ray diffraction (XRD), vibrating sample magnetometer (VSM), and X ray fluorescence (XRF) spectroscopy, respectively. The XRF measurement results found that the samples were composed of α-Fe_2O_3, TiO_2, SiO_2, and others. The crystallinity, magnetic, and composition properties of the samples were modified as milling time increases. The XRD patterns revealed that the samples have a hexagonal structure however, the crystalline size decreases with increasing milling time. The average crystallite size of iron oxide (α-Fe_2O_3), TiO_2, and α-Fe_2O_3/TiO_2 calculated based on Scherrer's formula was found to be 62.42nm, 37.12nm, and 49.77nm, respectively. The magnetic properties of the sample were studied through hysteresis loops measured using VSM to investigate the effect of milling time on the magnetic properties and found that all samples exhibited ferromagnetic behaviour with saturation magnetization (Ms) and remanence magnetization (Mr) increases to 63 and 74 %, respectively as milling time increases to 200h. The coercivity of the samples increases up to 360.10 Oe for the milling time of 100h and then decreases as the milling time increases. These coercivity values are smaller compared to that of pure hematite (α Fe_2O_3) nanoparticles. The α-Fe_2O_3/TiO_2 nanocomposites with controlled crystallite size and magnetic properties through different milling times may enable them to be used for environmental applications.

Keywords: logas natural sand, ball milling, iron oxide, titanium dioxide, and nanocomposite.

Manuscript Received 22 August 2024; Revised 9 December 2024; Published 10 January 2025

INTRODUCTION

Metal oxides such as Fe_2O_3, Fe_3O_4, TiO_2, ZnO, CuO, SnO_2dan $CeO_2$are oxides that have received a lot of attention from researchers, not only in fundamental properties but also in their technological applications ranging from high-density magnetic recording media to catalysts[1,2].Amongst these various metal oxide catalysts, iron oxide (α-Fe_2O_3) in controllable size has received considerable attention because of its broad range of applications. Metallic magnetic iron oxide shows promising catalytic activity because it is stable and has high specific surface area, and high crystallinity[3]. Therefore, α-Fe_2O_3 nanoparticles can be an alternative nanoparticle for environmental applications and wastewater treatment[4]. Apart from being stable, iron oxide (α-Fe_2O_3) nanoparticles are abundantly available in nature [5] and have a small energy band gap, namely 2.0-2.2 eV[6], so they can absorb visible light radiation. However, the catalytic activity of α-Fe_2O_3 iron oxide depends on the particle size. Various methods have been developed to obtain iron oxide nanoparticles with controlled sizes such as co-precipitation, hydrothermal[7], sol-gel [8] microwave [9], and ball milling[10,11]methods. However, to obtain iron oxide nanoparticles with controlled size, cheaply and efficiently, the ball milling method [12,13] can be used. Previous researchers [14,15] have used the ball milling method to prepare iron oxide nanoparticles. For example, researchers[15], prepared iron oxide nanoparticles directly from Logas natural sand-Kuansing District, Riau Province using the ball milling method and found that the ball milling product consisted of iron oxide (α-Fe_2O_3) nanoparticles with average crystallite size 39.2 nm.

The degradation efficiency of α-Fe_2O_3 iron oxide nanoparticles is reduced in water solution due to the agglomeration or large clusters due to dipolar attraction in magnetic iron oxide nanoparticles and thus reduces their specific properties of the nanoparticles. This is one of the weaknesses of α-Fe_2O_3 iron oxide nanoparticles as a catalyst. To overcome this weakness, previous researchers[16] used metal oxide nanoparticles such as titanium dioxide (TiO_2) to form a composite α-Fe_2O_3/TiO_2 with unique properties. For example, some researchers[17] recently used TiO_2/α-Fe_2O_3 composite which was prepared using the ball milling method, and applied it as a photocatalyst to degrade dyes with high degradation

efficiency[18]. Therefore, in this research α-Fe_2O_3/TiO_2 nanocomposite prepared from Logas natural sand, Kuansing district, Riau province using the ball milling method, and their structure, magnetic properties, and chemical composition were studied so that they could be used as a catalyst for the degradation of methylene blue dye.

EXPERIMENTAL PROCEDURE

Raw Material and Chemical

α-Fe_2O_3/TiO_2 nanocomposites were prepared from natural sand from Logas village-Kuansing District Riau Province. Pure hematite (α-Fe_2O_3) nanoparticles were purchased from TokoPedia (www.tokopedia.com).

Preparation of α-Fe_2O_3/TiO_2 Nanocomposites

α-Fe_2O_3/TiO_2 nanocomposites were prepared using Logas natural sand as raw material by ball milling method as the following steps: At first, the amount of non iron oxide particles of the samples was reduced using an ironsandseparator (ISS). The obtained iron oxide particles were then processed by a strong NdFeB magnet to separate between iron oxide and non-iron oxide particles before undergoing a 4-stage ball milled process with 15 milling balls of 20 mm-diameter iron balls in the vial. The first stage of milling lasted for 50 hours and was followed by separation between iron oxide and non-iron oxide using a strong NdFeB magnet. The second, third, and fourth stages of milling were carried out for 50 hours each and followed by separation between iron oxide and non-iron oxide using a strong NdFeB magnet for each stage. To investigate the influence of milling time on the α-Fe_2O_3/TiO_2 nanocomposite, pure hematite (α-Fe_2O_3) nanoparticles were used for comparison.

Characterization of α-Fe_2O_3/TiO_2 Nanocomposites

The prepared samples were examined by XRD, VSM, and XRF to study their structural, magnetic, and compositional properties. The structural properties of the samples were examined by X-ray diffraction (XRD; PAN analytical Xpert Pro.) equipped with Cu-Kα Radiation in the range of 10-100°. To analyse the magnetic properties, the samples were examined by a vibration sample magnetometer (VSM). The chemical compositions of the prepared nanocomposites were examined by X-ray fluorescence (XRF) spectroscopy. In this research, pure α-Fe_2O_3 nanoparticles were used for comparison.

RESULTS AND DISCUSSIONS

Structural Analysis

The XRD patterns of α- Fe_2O_3/TiO_2 nanocomposite are displayed in Figure-1. The nanocomposite patterns revealed 9 main diffraction peaks at 2θ = 23.968°, 32.773°, 35.381°, 40.496°, 49.019°, 53.424°, 61.824°, 63.481°, and 70.786° for milling time of 50 h. These diffraction peaks were due to the crystal plane of the hematite structure (102), (104), (110), (113), (024), (116), (122), (214), (300), and (119) planes. The α-Fe_2O_3/TiO_2 nanocomposite was found to have the same crystal planes of hexagonal α-Fe_2O_3[13] which is in good agreement with the JCPDS (Joint Committee on Powder Diffraction Standards) data file No. JCPDS: 33-0664[19]. However, the effect of increasing milling time shifts the diffraction peaks towards the slightly lower diffraction angle region as shown in Figure-2. An additional peak of TiO_2 confirms the formation of α- Fe_2O_3/TiO_2 nanocomposite with a high degree of crystallinity revealed by sharp and narrow diffraction peaks. It was shown in Figure-2 that with increased milling time, the increased peak width indicates reduced crystallite size. The expanded XRD patterns of α-Fe_2O_3/TiO_2 nanocomposite in the range from 2θ = 32.4° to 33.6° show clear a shift in the diffraction peak positions compared to that for pure α-Fe_2O_3 nanoparticles.

The average crystallite size of prepared nanocomposites was determined by observing all the maximum intensity peaks in the XRD pattern using Scherrer's formula ($D = K\lambda/\beta\cos\theta$) [20]. Here K is the Scherrer's factor (0.9), λ is the wavelength of incident X-rays, β is the FWHM and θ is the Bragg's diffraction angle for the observed peak. In addition to all diffraction peaks of α- Fe_2O_3, another diffraction peak appeared at 37.313° which corresponded to the (004) plane of TiO_2 (JCPDS file No 21-1272).Moreover, another diffraction peak at 2θ= 25.61° corresponds to the (111) plane of silicon. XRD results demonstrated that the crystalline TiO_2 and α-Fe_2O_3 coexisted in α-Fe_2O_3/TiO_2 nanocomposite. The average crystallite sizes for α-Fe_2O_3 nanoparticles were found to decrease as milling time increased as indicated in Figure-3.The average crystallite size of TiO_2 is 37.12 nm. The average crystallite size of α-Fe_2O_3/TiO_2 nanocomposite and TiO_2 nanoparticles is smaller than that for iron oxide α-Fe_2O_3.

The results revealed that the intensity peaks of the TiO_2 peaks appear to be quite low when the milling time increases and the peak's intensity increases slightly. Moreover, the intensity of α-Fe_2O_3 peaks increases as milling time increases. The XRD patterns indicated that the α-Fe_2O_3 nanoparticles have an average crystallite size of 62.42 nm and based on the dominant peak (104) the average crystallite size is 52.31 as shown in Table-1. The decrease in the degree of agglomeration among iron oxide (α-Fe_2O_3) nanoparticles is due to the increase in milling time. This is one of the responsible parameters to produce the smaller size of iron oxide (α- Fe_2O_3)/TiO_2 nanocomposite. The chemical composition of the samples is presented in Table-2. It can be seen that the XRF data evidence the occurrence of TiO_2. The table also indicates that the α-Fe_2O_3/TiO_2 nanocomposite is not free from impurity elements such as SiO_2.

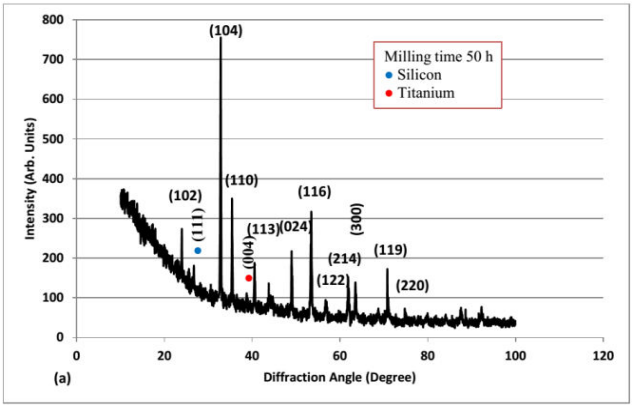

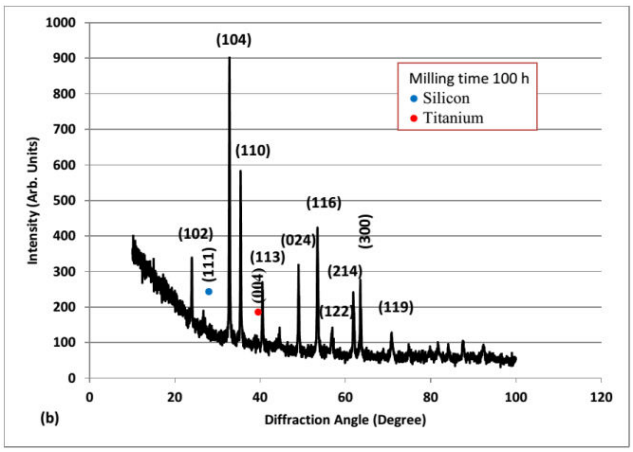

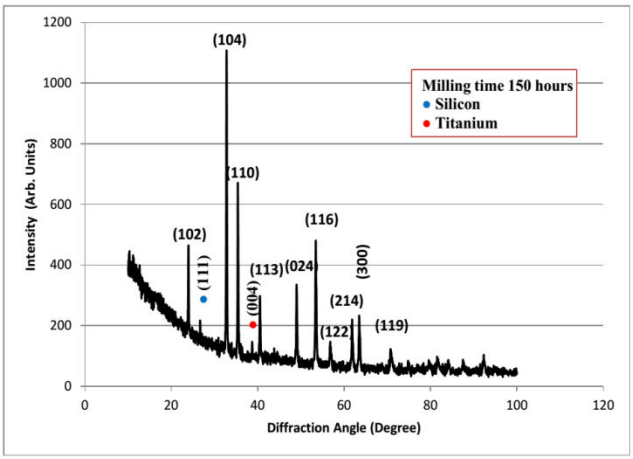

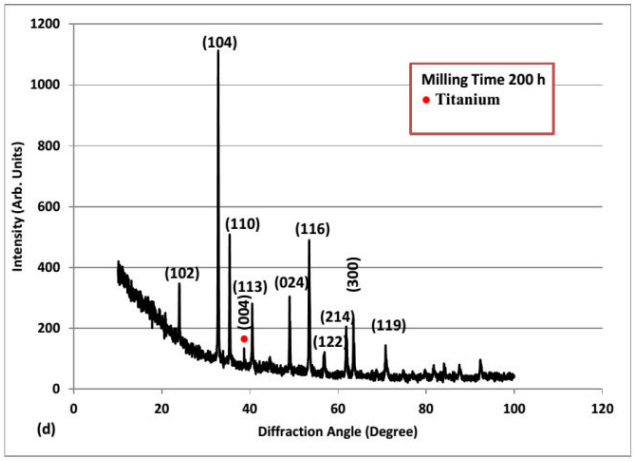

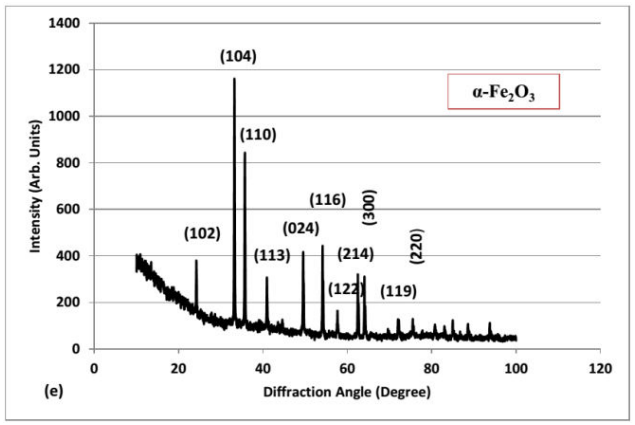

Figure-1.X-ray diffraction patterns of α-Fe_2O_3/TiO_2 nanocomposite for different milling times and pure hematite (α-Fe_2O_3) nanoparticles for comparison.

Table-1. Average crystallite size of α- Fe_2O_3, TiO_2, and α- Fe_2O_3/TiO_2 nanocomposite.

Sample	Average Crystallite size of all peaks (nm)	Average Crystallite size peak (104) (nm)
α- Fe_2O_3	62.42	52.31
TiO_2	37.12	-
α- Fe_2O_3/TiO_2	49.77	-

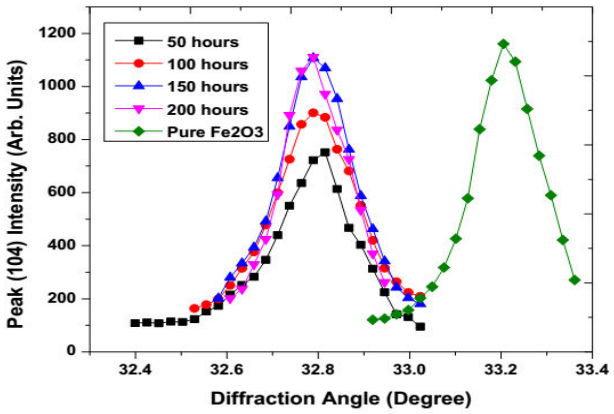

Figure-2. Expanded diffraction angle of peak (104) α-Fe_2O_3/TiO_2 nanocomposite for different milling times showing a shift of peak position to slightly lower diffraction angle and pure α-Fe_2O_3 for comparison.

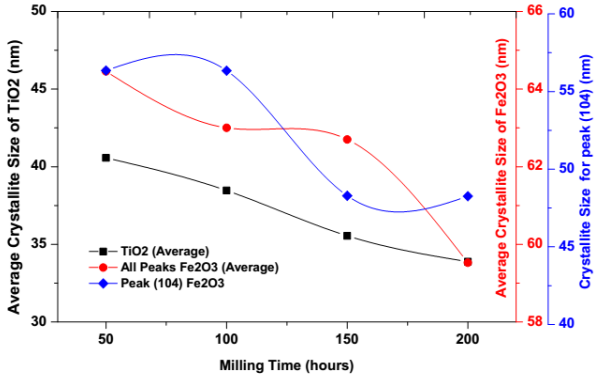

Figure-3. The average crystallite size of α-Fe_2O_3 based on all peaks, peak (104), and crystallite size of TiO_2 as a function of milling time.

Table-2. Concentration of iron oxide (α-Fe_2O_3), TiO_2, SiO_2 and other nanoparticles in the samples for different milling time.

Milling Time (hours)	α-Fe_2O_3 (%)	TiO_2 (%)	SiO_2 (%)	Others (%)
50	32.328	25.818	31.598	10.256
100	41.835	28.582	21.243	8.340
150	42.863	30.562	18.262	8.313
200	53.274	40.464	0.924	5.338

Magnetic Properties

The magnetic properties of the α-Fe_2O_3/TiO_2 nanocomposites have been studied through their hysteresis loops measured using a vibration sample magnetometer (VSM). The applied magnetic field used in this measurement sweeps from - 20 to 20 kOe. As shown in Figure-4, the magnetization measurement results of all the samples show the presence of ferromagnetic behaviour characterized by their low coercivity value. The hysteresis loops analysis shows that the saturation magnetization (Ms) and remanent magnetization (Mr) values increase with increasing the applied magnetic field and reach the saturation value under a high applied magnetic field of 20 kOe, which agrees with previous observations in earlier works[21]. The magnetic parameters consisting of Ms, Mr, and Hc of the prepared α-Fe_2O_3/TiO_2 nanocomposites are shown in Figure-5. The increase of Ms Value with increasing milling time might be because of the increasing amount of α-Fe_2O_3 which contributes to the magnetization value of the samples. The increasing amount of α-Fe_2O_3 leads to a higher magnetic moment per unit mass. The saturation magnetization of α-Fe_2O_3/TiO_2 nanocomposite is in good agreement with those reported by previous researchers[22].

The coercivity of the α-Fe_2O_3/TiO_2 prepared with a milling time of 50 h is about 349.42Oe and increases to 360.10Oe and then decreases to 357.94 and 88.50Oe with increasing milling time of 100, 150 and 200h, respectively. Thus the increase of coercivity in this range (50 to 100h) of milling time can be qualitatively understood in terms of the effect of more segregation among oxide nanoparticles, which ultimately reduces exchange coupling between weakly coupled iron oxide nanoparticles or clusters[23]. Furthermore, magnetization data are smaller than those of pure Fe_2O_3 nanoparticles as indicated in Figure-6. The magnetic data of Fe_2O_3 nanoparticles are Ms = 0.899 emu/g, H_C=1397.71Oe. Comparing these data indicates that all α-Fe_2O_3/TiO_2 nanocomposites exhibit high saturation magnetization compared to that of pureα-Fe_2O_3 nanoparticles, which is related to the high magnetization of other atoms in the samples. However, α-Fe_2O_3/TiO_2 nanocomposite derived from Logas natural sand has smaller coercivity (Hc) values as compared to that of pure α-Fe_2O_3 nanoparticles, which proved their better superparamagnetic behaviour. Hence, it can be concluded that the α-Fe_2O_3/TiO_2 nanocomposite improves its superparamagnetic properties.

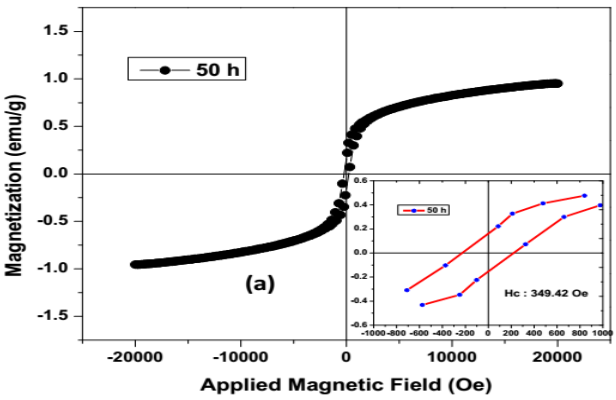

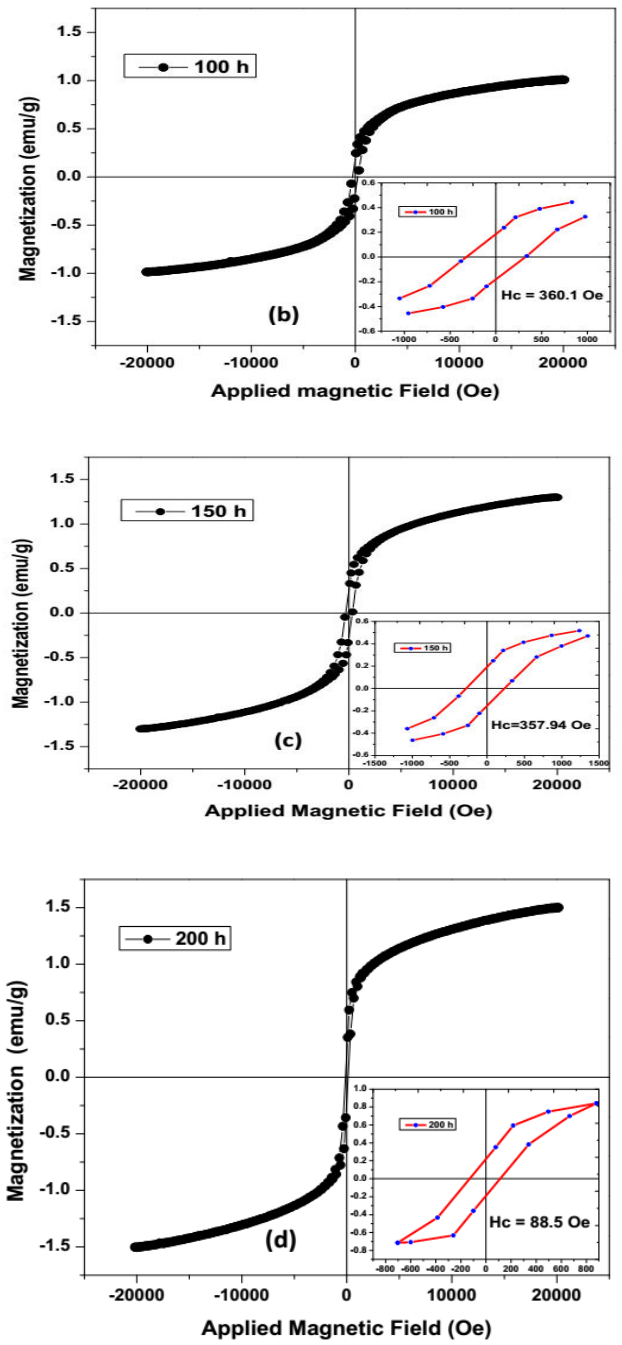

Figure-4. Hysteresis loops of α-Fe_2O_3/TiO_2nano composite with different milling times and the inset showing the enlarged loop of the samples.

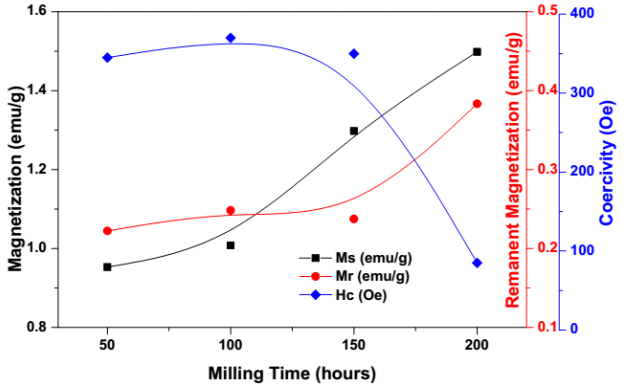

Figure-5. Saturation magnetization (Ms), remanent magnetization (Mr), and coercivity (Hc) of α-Fe_2O_3/TiO_2 nanocomposite as a function of milling time.

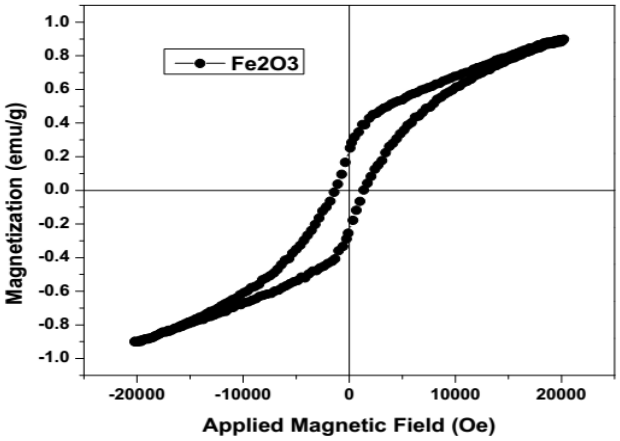

Figure-6. Hysteresis loop of pure hematite (α-Fe_2O_3) nanoparticles.

CONCLUSIONS

In this study, α-Fe_2O_3/TiO_2 nanocomposites were prepared by milling method. The XRD measurement revealed that the sample has a hematite phase with a high degree of crystalline. The measurements also confirmed the crystallite size decreases as milling time increases. The results of the VSM analysis showed that increasing milling time from 50h to 200h caused 63% and 74% increase in the saturation magnetization and remanence magnetization values, respectively. The coercivity of the samples increases with increasing milling time up to 100h and decreases rapidly after 150h. The XRF study showed that the samples are not free from impurity elements such as SiO_2. The ability to modify α-Fe_2O_3/TiO_2 nanocomposites with controlled crystallite size through different milling times may enable them to be used for environmental applications.

ACKNOWLEDGMENTS

Authors gratefully acknowledge financial support from the Directorate General of Higher Education, Indonesian Ministry of Education, Culture, Research and Technology (Agreement no. 085/E5/PG.02.00.PL/2024).

The authors are grateful to the National Innovation Research Agency (BRIN), for conducting the VSM measurement and the Department of Physics and Chemistry UNP for conducting the XRD and XRF measurements. The authors also thank magnetic research members in Magnetism Laboratory FMIPA UNRI, for their assistance during sample collection and preparation.

REFERENCES

[1] Frey N. A., Peng S., Cheng K., Sun S. 209. Magnetic nanoparticles: Synthesis, functionalization, and applications in bio imaging and magnetic energy storage. Chem. Soc. Rev.38, pp. 2532-2542.

[2] Zhiqin Cao, Mingli Qin, Yueru Gu, BaoruiJia, Pengqi Chen, Xuanhui Qu. 2016. Synthesis and characterization of Sn doped hematite as a visible light photocatalyst, Mater. Res. Bull. 77: 41-47.

[3] B. Silke and A. Ingo. 2016. Manetic Nanocomposites. Current opinion in Biotechnology. 06, 39, 89-96.

[4] Pegu R., Majumdar K. J., Talukdar D. J., Pratihar S. 2014. Oxalate capped iron nanomaterial: from methylene blue degradation to bis (indolyl) methane synthesis.Rsc. Advances. 4: 33446-33456.

[5] Erwin Amiruddin, Amir Awaluddin, Meilan Sihombing, Azura Royka and Tissa Syahrul. 2020. Morphology and structural properties of undoped and cobalt doped magnetic iron oxide particles for improving the environmental quality. International Journal of Engineering and Advanced Technology (IJEAT). 9(6): 18-21.

[6] Gilbert B., Frandsen C., Maxey er, Sherman D. M. 2009. Band-gap measurements of bulk and nanoscale hematite by soft X-ray spectroscopy. Phys rev B 79: 35108-1-35108-7

[7] Tadica M., Panjan M., Damnjanovicc V., Milosevic I. 2014. Magnetic properties of hematite (α-Fe_2O_3) nanoparticles prepared by hydrothermal synthesis method. Appl Surf Sci. 320, 183-7.

[8] N. Abbas, G. N. Shao, M. S. Haider, S. M. Imran, S. S. Park, H. T. Kim. 2016. Sol-gel synthesis of TiO_2-Fe_2O_3 systems: Effects of Fe_2O_3 content and their photocatalytic properties J. Ind. Eng. Chem. 39, 112120.

[9] L. Hu, A. Percheron, D. Chaumont. 2011. Microwave-assisted one-step hydrothermal synthesis of pure iron oxide nanoparticles: magnetite, maghemite, and hematite. 198-205.

[10] A. Erwin, S. Salomo, P. Adhy, N. Utari, W. Ayu, Y. Wita and S. Nani. 2020. Magnetic iron oxide particles (Fe_3O_4) are fabricated by ball milling to improve the environmental quality. IOP Conf. Series: Materials Science and Engineering. 845: 012051.

[11] S. Razavi-Tousi and J. Szpunar. 2015. Effect of ball size on the steady state of aluminum powder and efficiency of impacts during milling. Powder Technology. 284: 149-158.

[12] Erwin Amiruddin, Salomo Sinuraya, Amir Awaluddin, Martha Rianna, Heri Hadianto, Muhammad Rizki, Novia Magdalena Purba and Indah Tamara Sitorus. 2023. Chromium Doped Iron Oxide Nanoparticles and Physical Properties Prepared from Logas Natural Sand and Their Application in Photo-Fenton Degradation of Methylene Blue Dye. ARPN Journal of Engineering and Applied Sciences. 18(10): 1102-1110.

[13] B. Sharma, P. K. Boruah, A. Yadav and M. R. Das, 2018. TiO_2–Fe_2O_3 nanocomposite heterojunction for superior charge separation and the photocatalytic inactivation of pathogenic bacteria in water under direct sunlight irradiation, J. Environ. Chem. Eng., 6(1): 134-145, doi: 10.1016/j.jece.2017.11.025.

[14] Erwin Amiruddin, Amir Awaluddin, Innike Hariani, Ribka Sihombing and Riska Angraini. 2020. The Influence of Milling Ball Size on the Structural, Morphological, and Catalytic Properties of Magnetite (Fe_3O_4) Nanoparticles toward Methylene Blue Degradation. Journal of Physics: Conference Series 1655. 012006 doi:10.1088/1742-6596/1655/1/012006

[15] Heri Hadianto, Erwin Amiruddin, Rebi Septiawan, Putri Venera and Vivi Aprilia. 2020. Structural and Morphological Properties of Undoped and Manganese Doped Hematite Nanoparticles Prepared by Ball Milling Method. Journal of Physics: Conference Series 1655. 012013doi:10.1088/1742-6596/1655/1/012013

[16] Baldrian P., Merhautova V., Gabriel J., Nerud F., Stopka P. 2006. Decolorization of synthetic dyes by hydrogen peroxide with heterogeneous catalysis by mixed iron oxides. Appl. Catal. B 66: 258-264.

[17] S. Lubis, I. Maulana and M. 2018. Synthesis and Characterization of TiO_2/α-Fe_2O_3 Composite using Hematite from Iron Sand for Photodegradation Removal of Dye. J. Nat. 18(1): 38-43,doi: 10.24815/jn.v18i1.8649.

[18] S. C. Lee, H. O. Lintang and L. Yuliati. 2017. High photocatalytic activity of Fe_2O_3/TiO_2 nanocomposites prepared by photodeposition for degradation of 2, 4-dichlorophenoxyacetic acid. Beilstein J. Nanotechnol., 8(1): 915-926, doi: 10.3762/bjnano.8.93.

[19] Xuehui Rao, Xintai Su, Chao Yang, Jide Wang, Xinping Zhen, and Daishun Ling. 2013.From spindle-like b-FeOOH nanoparticles to a-Fe_2O_3 polyhedral crystals: shape evolution, growth mechanism, and gas sensing property. Cryst Eng Comm. 15, 7250.

[20] B. D. Cullity. 1978. Elements of X-Ray Diffraction (Addison-Wesley, Boston). p. 102.

[21] Erwin Amiruddin, Salomo Sinuraya, Rahmondia N. Septiadi, Yanuar Hamzah, Amir Awaluddin, Loly A. Hardani, Fitri A. Lestari, Yessi Magdalena and Devi T. Gurning. 2022. A Systematic Study of the Structural and Magnetic Properties of Nickel Doped α-Fe_2O_3Nanoparticles Prepared from Logas Natural Sand. ARPN Journal of Engineering and Applied Sciences. 17(14): 1408-1413.

[22] Houda Mansour, K. Omri, Radhouane Bargougui, Salah Ammar. 2020. Novel α-Fe_2O_3/TiO_2 nanocomposites with enhanced photocatalytic activity. Applied Physics A. 126:151 https://doi.org/10.1007/s00339-020-3320-3

[23] Erwin and Adhy Pryayitno. 2017. Magnetic exchange interaction in cobalt samarium thin films for high-density magnetic recording media. ARPN Journal of Engineering and Applied Sciences. 12, 12, 3832-3835.